Basigin-2 Is a Cell Surface Receptor for Soluble Basigin Ligand*⒮

Robert J. Belton, Jr.,[1] **Li Chen, Fernando S. Mesquita, and Romana A. Nowak**

From the Department of Animal Sciences, University of Illinois at Urbana-Champaign, Urbana, Illinois 61801

The metastatic spread of a tumor is dependent upon the ability of the tumor to stimulate surrounding stromal cells to express enzymes required for tissue remodeling. The immunoglobulin superfamily protein basigin (EMMPRIN/CD147) is a cell surface glycoprotein expressed by tumor cells that stimulates matrix metalloproteinase and vascular endothelial growth factor expression in stromal cells. The ability of basigin to stimulate expression of molecules involved in tissue remodeling and angiogenesis makes basigin a potential target for the development of strategies to block metastasis. However, the identity of the cell surface receptor for basigin remains controversial. The goal of this study was to determine the identity of the receptor for basigin. Using a novel recombinant basigin protein (rBSG) corresponding to the extracellular domain of basigin, it was demonstrated that the native, nonglycosylated rBSG protein forms dimers in solution. Furthermore, rBSG binds to the surface of uterine fibroblasts, activates the ERK1/2 signaling pathway, and induces expression of matrix metalloproteinases 1, 2, and 3. Proteins that interact with rBSG were isolated using a biotin label transfer technique and sequenced by matrix-assisted laser desorption ionization tandem mass spectrophotometry. The results demonstrate that rBSG interacts with basigin expressed on the surface of fibroblasts and is subsequently internalized. During internalization, rBSG associates with a novel form of human basigin (basigin-3). It was concluded that cell surface basigin functions as a membrane receptor for soluble basigin and this homophilic interaction is not dependent upon glycosylation of the basigin ligand.

The metastatic spread of cancer cells within host tissue is dependent upon the local microenvironment surrounding the primary tumor. Within this microenvironment, cancer cells stimulate surrounding stromal cells to express factors required for remodeling of the host tissue, thus allowing for the survival, proliferation, and metastasis of the tumor (1). Therefore, an understanding of the molecules mediating tumor-stromal cell interactions is critical for the development of strategies needed to diagnose and treat metastatic cancers. This need is underscored by the fact that many molecules identified as biological markers for metastatic cells are also expressed by host cells

under normal physiological conditions (2). One particularly good example of such a molecule is the cell surface glycoprotein basigin. Basigin is an integral membrane glycoprotein belonging to the immunoglobulin superfamily, and it is expressed on numerous cell types (reviewed in Refs. 2–4). Originally identified in LX-1 lung carcinoma cells as a secreted factor capable of stimulating the collagenase activity of human fibroblasts, basigin has been identified independently in several different model systems resulting in a long list of acronyms for this molecule including tumor collagenase stimulatory factor (5–7), EMMPRIN (8), neurothelin (9), OX-47 (10), gp42 (11), CE9 (12), 5A11 (13), HT7 (14), M6 (15), OK blood antigen (16), and most recently CD147 (17). Basigin is the approved HUGO Gene Nomenclature Committee designation for the human gene and will be used to refer to the gene sequence and the expressed proteins in this paper.

Human basigin is expressed as two differentially spliced isoforms encoded by a single gene found on chromosome 19p13.3 (18–20). The molecule is characterized by the presence of two extracellular immunoglobulin-like domains, a single transmembrane domain possessing a charged amino acid, and a short cytoplasmic tail containing a basolateral membrane-targeting motif (21, 22). The more recently identified retina-specific isoform of basigin is distinguished by an additional immunoglobulin-like sequence in the extracellular domain of the protein (20, 23). According to the current naming system of the National Center for Biotechnology Information, the larger retina-specific isoform has been renamed basigin-1 (accession number NM_001728.2), and the prototypical isoform, possessing two immunoglobulin domains, has been renamed basigin-2 (accession number NM_198589.1). Both basigin isoforms are variably glycosylated on asparagine residues, which results in significant alterations in their relative molecular weights depending upon the extent of β1,6-branched polylactosamine incorporation during transit of the protein through the Golgi (23, 24).

Several functions have been described for basigin within both normal and malignant tissues. The best characterized function for basigin is its ability to induce the expression of matrix metalloproteinases (MMPs)[2] in stromal cells. Studies using tumor cell-stromal cell co-culture systems, or the treatment of stromal cells with soluble basigin protein demonstrated that basigin stimulates expression of several MMPs including MMP-1, -2,

[2] The abbreviations used are: MMP, matrix metalloproteinase; EMMPRIN, extracellular matrix metalloproteinase inhibitor; rBSG, recombinant basigin; TIMP, tissue inhibitor of metalloproteinases; HESC, human endometrial stromal cell; HRP, horseradish peroxidase; siRNA, small interfering RNA; ERK, extracellular signal-regulated kinase; MALDI, matrix-assisted laser desorption ionization; MS/MS, tandem mass spectrophotometry; PFO, perfluorooctanoate; pAb, polyclonal antibody; EGF, epidermal growth factor.

TABLE 1
Oligonucleotide primers used in this study

Open reading frame forward	5′–ATGGTAGGTCTCAGCGCCGCCGGCACAGTCTTCACTACC–3′
Open reading frame reverse	5′–ATGGTAGGTCTCAGGCCCAGGTGGCTGCGCACGCGG–3′
Primer a	5′–CGGCTTAGTCTGCGGTCC–3′
Primer e	5′–GCGGTTGGAGGTTGTAGGAC–3′
Primer f	5′–TCCGACTGCTTCATTGTGGG–3′
Primer g	5′–GGGAGGAAGACGCAGGAGTA–3′
Primer h	5′–TTTTTTGAGGGTGGAGGTGG–3′

and -3 (reviewed in Ref. 2). Evidence that cancer cells overexpress basigin and shed microvesicles containing basigin protein supports the hypothesis that tumors can modify their local microenvironment by altering the balance between the expression level of MMPs and their physiological inhibitors, the tissue inhibitors of matrix metalloproteinases (25, 26). Despite a growing understanding of basigin function in tumor-stromal cell interactions, it remains unclear what protein on the surface of stromal cells functions as the receptor for basigin. Transfection of COS cells with a recombinant form of human basigin demonstrated that basigin can mediate cell adhesion events (27). Homophilic interactions have been demonstrated for other immunoglobulin superfamily proteins including intercellular adhesion molecules (28), neural cell adhesion molecules (29), and cadherins (30). However, attempts to demonstrate specific homophilic interactions between basigin molecules expressed on separate cells or between soluble forms of recombinant basigin using surface plasmon resonance have not been successful, suggesting that basigin-2 cannot function as a receptor for itself (20, 31).

To identify possible receptors for soluble basigin ligand, an affinity purification approach was employed. Human uterine fibroblasts were treated with a novel recombinant basigin-2 protein (rBSG) consisting of the extracellular domain of basigin-2. This purified protein possesses a stable folded structure and forms dimers in solution. Treatment of uterine fibroblasts with rBSG activated the ERK1/2 signaling pathway and stimulated the expression of MMP-1, MMP-2, and MMP-3 in a dose-dependent manner. Identification of rBSG receptors was performed using a biotin label transfer method where intact cells were treated with rBSG conjugated to the heterotrifunctional cross-linking agent Sulfo-SBED. This approach resulted in the labeling of several potential interacting proteins, and MALDI-MS/MS sequencing of one of these proteins identified a novel isoform of human basigin (basigin-3). Immunoprecipitation studies using cell fractions revealed that rBSG interacts with basigin-2 at the cell membrane and subsequently interacts with the basigin-3 isoform within the cell. Small interfering RNA (siRNA) knockdown of basigin-2 protein reduced, but did not eliminate, rBSG-mediated ERK activation in HESCs, suggesting that additional cell surface receptors for soluble basigin may exist. Taken together, these results support the hypothesis that basigin-2 can function as a receptor for soluble basigin and demonstrate that the homophilic interactions between basigin proteins are not dependent upon glycosylation of the basigin ligand.

EXPERIMENTAL PROCEDURES

Cell Lines and Reagents—Immortalized HESCs were a gift of Dr. Charles Lockwood (Yale University) and were cultured as described by Krikun *et al.* (32). The human cervical carcinoma cell lines CCL-2 (HeLa), C4-I, and C4-II were purchased from American Type Culture Collection and cultured using the protocols provided. Full-length human basigin-2 in the pBluescript II plasmid was a gift from Dr. Muramatsu (Kagoshima University, Kagoshima, Japan). The P2C2 basigin monoclonal antibody was generated with assistance from the University of Illinois Immunological Resource Center (supplemental Fig. S1). The pASK_IBA44 bacterial expression vector was from IBA. Custom oligonucleotide primers were purchased from Integrated DNA Technologies, Inc. The ERK1/2 antibodies and HRP-conjugated secondary antibodies were from Cell Signaling. Restriction endonucleases, phosphatase, and ligase reagents were from New England Biolabs. The anti-rabbit HRP-conjugated secondary antibody (anti-human, anti-mouse depleted) was from Santa Cruz Laboratories. The anti-human EMMPRIN polyclonal antibody (pAb) was from R & D Technologies. *Pfu* ultra polymerase and BL21-RP Codon-plus *Escherichia coli* were from Stratagene. The caveolin-1, SOS, and HIM6 antibodies and Superscript III reverse transcriptase were from Invitrogen. The Sulfo-SBED biotin label transfer kit, D-Salt dextran columns, neutravidin ultralink and protein G beads, and Pico chemiluminescent detection reagent were from Pierce. PrimeStar HS polymerase was from Takara Mirus. TaqMan® universal PCR Master Mix, 20×Assays-On-Demand and MicroAmp optical 384-well reaction plates were from Applied Biosystems.

Generation and Purification of rBSG—The extracellular domain of human basigin, corresponding to amino acids 23–206 of isoform 2, was amplified by high fidelity PCR amplification using the open reading frame forward and reverse primers (Table 1). The resulting PCR product was ligated into the BsaI linearized pASK_IBA44 vector, and the DNA sequence of the construct was determined at the Keck Biotechnology Center at the University of Illinois.

For recombinant protein expression, the IBA44-rBSG construct was transformed into the BL21-RP CodonPlus strain of *E. coli*. Single bacterial colonies were inoculated into SOC medium (2% tryptone, 0.5% yeast extract, 8.6 mM NaCl, 10 mM MgCl2, 10 mM MgSO4, 20 mM glucose) containing ampicillin and chloramphenicol (SOC/A/C). The cultures were grown for 6 h at 37 °C, 250 RPM, diluted 1/100 into SOC/A/C, and grown for 12–14 h at 25 °C, 250 RPM. The cultures were diluted ⅕ into SOC/A, grown until the A_{550} was >0.8, and protein expression was induced with the addition of 0.2 μg/ml anhydrotetracycline. Following 6 h of induction, detergent free osmotic shock lysate was generated according to standard methods. Briefly, bacteria were resuspended in 80 ml/gram of wet weight of ice-cold sucrose buffer (20% sucrose, 30 mM Tris, pH 8), 1 mM EDTA was added dropwise, and the cells were incubated on ice for 10 min. The cells were collected by centrifugation at 8000 × *g* 20 min at 4 °C, the sucrose buffer was discarded, and the

bacteria was resuspended in 5 mM $MgSO_4$. Following centrifugation at 8000 $\times$ *g* for 20 min, the osmotic shock lysate was filtered through a 0.22-μm cellulose acetate filter to remove cellular debris, concentrated 250-fold using 10-kDa centrifugal filters, and dialyzed into wash buffer (300 mM NaCl, 50 mM NaH_2PO_4, pH 8). The osmotic shock lysate from 1 liter of culture was incubated with 1 ml of Talon metal affinity beads (Amersham Biosciences) for 90 min at 4 °C. The bound protein was washed with >30 bed volumes of wash buffer, followed by 10 bed volumes of wash buffer containing 5 mM imidazole. The recombinant protein was eluted with 10 bed volumes of wash buffer containing 200 mM imidazole. The eluted protein was dialyzed into phosphate-buffered saline and characterized by SDS-PAGE, PFO-PAGE, and immunoblotting.

PFO-PAGE—rBSG protein was analyzed by PFO-PAGE as described by Ramjeesingh *et al.* (33). The purified rBSG protein was diluted into PFO-PAGE sample buffer (50 mM Tris, pH 8, 10% glycerol, 4% PFO) and loaded onto an 8% native polyacrylamide gel that had been prerun for 45 min at 50 volts in PFO running buffer (25 mM Tris, pH 8, 192 mM glycine, 0.5% PFO).

Endotoxin Analysis of rBSG—The measurement of bacterial endotoxin present in the purified rBSG was performed by Cambrex Bioscience Walkersville, Inc. (Walkersville, MD) using the limulus amoebocyte lysate assay. 100 μg/ml of rBSG was analyzed following established Food and Drug Administration guidelines (SOP 162.6).

Quantitative Real Time PCR Analysis—HESCs grown to 90% confluency in 10-cm dishes were treated with rBSG at 0.1, 1, 10, and 100 μg/ml for 24 h in serum-free Dulbecco's modified Eagle's medium/F-12 at 37 °C. Total RNA was isolated using the TRIzol method, reversed transcribed into cDNA, and analyzed by real time PCR using TaqMan® Universal PCR Master Mix. MMP-1, MMP-2, MMP-3, and glyceraldehyde-3-phosphate dehydrogenase sequences were amplified using the 20xAssays-on-Demand™ gene expression assay. Real time PCR amplification and detection was performed in MicroAmp optical 384-well reaction plates using the ABI 7900 sequence detection system. Relative fold differences between the tested genes were obtained by the comparative Ct method. To show changes in gene expression relative to control level (control set as 1), each biological replicate was normalized to the average of the control group within each experiment. Relative fold difference values for each experiment were checked for normality and common variances, respecting the assumptions for performing analysis of variance. All of the distributions were normal, and the experiments with unequal variances were analyzed by Welch's analysis of variance. A completely randomized design corresponding to the following linear model was used: $X_{ij} = \mu + \tau_i + \epsilon_{ij}$, where X_{ij} is an observation, μ is the population mean, τ_i is the effect of *i*th treatment, and ϵ_{ij} is an error term. Post hoc comparisons using Tukey's procedure ($\alpha = 0.05$) were only performed when analysis of variance indicated significant effect caused by treatment. The data analysis for this paper was generated using SAS software (Copyright, SAS Institute Inc.).

Collection of Cell Lysates and Cell Fractions—Soluble cell lysates were collected in ice-cold immunoprecipitation buffer (1% Nonidet P-40, 0.5% deoxycholate, 0.1% SDS, 20 mM HEPES, pH7.4, 150 mM NaCl, 1 mM EDTA, 1 mM Na_3VO_4, 1 mM NaF,

10% glycerol, 0.5 mM phenylmethylsulfonyl fluoride, protease inhibitors). The lysates were incubated on ice for 30 min and centrifuged at 20,000 $\times$ *g* for 15 min 4 °C, and the soluble fraction was collected. For cell fractionation studies, the cells were harvested by scraping cells into ice-cold hypo-osmotic buffer (10 mM Tris, pH 7.4, 2 mM EDTA, protease inhibitor mixture), sonicated for 5 s, and spun at 500 $\times$ *g* for 10 min at 4 °C to remove nuclei and cell debris. The supernatant was transferred to a Beckman SW-55Ti rotor and centrifuged at 100,000 $\times$ *g* for 15 min 4 °C. The soluble cytoplasmic fraction was collected, and the remaining membrane pellet was solubilized in immunoprecipitation buffer. Protein concentration determination was performed using the BCA method.

Immunoprecipitation and Immunoblot Analysis—Immunoprecipitation of basigin was performed using the monoclonal antibody P2C2 (see supplemental data). 10–15 μg of antibody added to 1 mg of soluble protein was incubated overnight at 4 °C with rocking, and immune complexes were collected on protein G-Sepharose beads for 4 h at 4 °C. Immunoprecipitated proteins were resolved by SDS-PAGE using standard methods. For immunoblotting, SDS-PAGE gels were transferred to nitrocellulose, blocked in TBST (20 mM Tris, pH 8, 150 mM NaCl, 0.1% Tween 20) containing 5% nonfat dry milk for 60 min at room temperature and incubated with primary antibodies as indicated. HRP-conjugated secondary antibodies were used at a dilution of 1:15,000. The blots were washed, and the bands were visualized using the Pierce Pico chemiluminescence reagent.

siRNA Knockdown of Basigin—Basigin protein expression was knocked down by reverse transfection using the basigin Silencer® small interfering RNA oligonucleotide and the siPORT™ amine transfection reagent according to the manufacturer's recommendations (Ambion). Proliferating HESCs were harvested and 80,000 cells plated in 12-well dishes containing 60 nM oligonucleotide. Control transfections used the Silencer® negative control #1 siRNA. The medium was replaced 48 h post-transfection, and the cells were treated with 10 μg/ml rBSG or 100 ng/ml recombinant human EGF for the times indicated. The cell lysates were collected by the addition of 100 μl of boiling 2% SDS, 62 mM Tris, pH 6.8, 10% glycerol.

Biotin Label Transfer and Protein Purification—Purified rBSG was labeled with the heterotrifunctional cross-linking reagent Sulfo-SBED according to the manufacturer's recommendations. For this, rBSG protein was combined with the Sulfo-SBED label transfer reagent at a molar ration of 1:4 in the dark at 4 °C for 2 h. Unincorporated Sulfo-SBED was removed by gel filtration on D-Salt dextran desalting columns. Labeled rBSG was diluted into prewarmed, serum-free culture medium and added to the cells. The cells were incubated with the labeled protein at 37 °C in the dark for 10 min and cross-linked using a Stratalinker UV light source for 5 min. The medium was aspirated, and the HESCs were washed twice with phosphate-buffered saline. Soluble cell lysate from 5 $\times$ 10^7 cells was prepared and applied to a 1-ml bed of Monomeric Avidin Ultralink beads (Pierce) for 1 h at 4 °C, and the column was washed with 20 volumes of column buffer (1$\times$ phosphate-buffered saline, pH 7.4, 1 mM EDTA, 0.05% Tween 20). The rBSG ligand was eluted from the column with 5 bed volumes of column buffer containing 50 mM dithiothreitol. All of the remaining biotinylated pro-
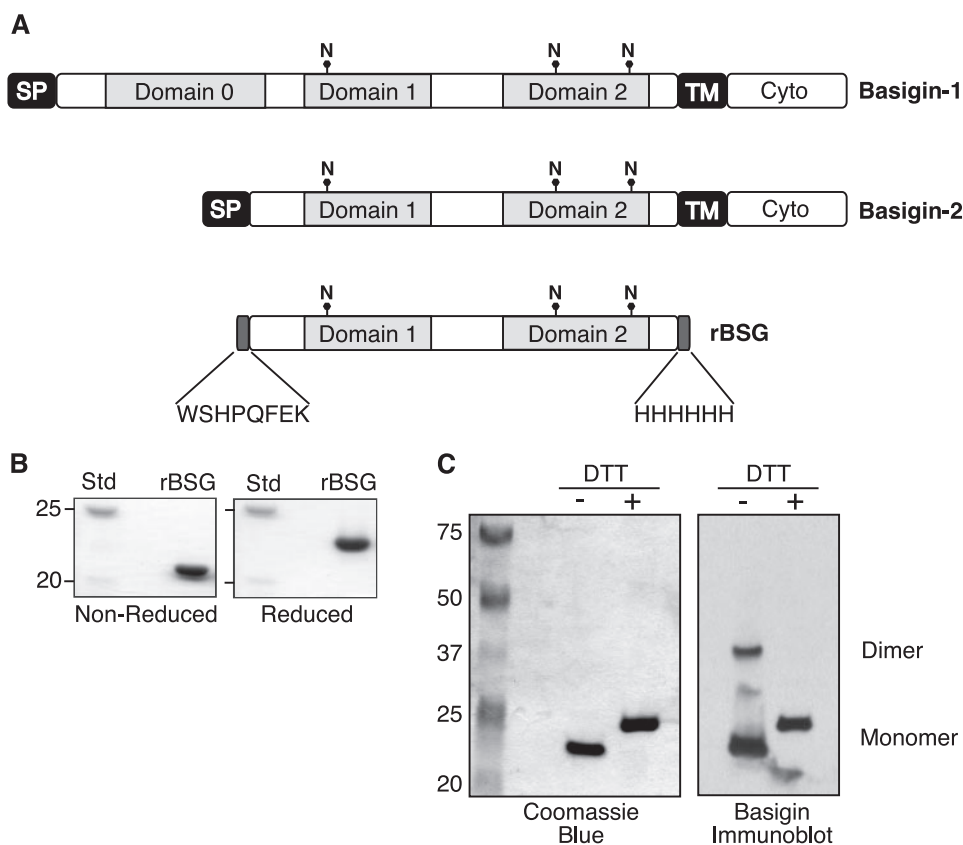
A

B

C

FIGURE 1. **Recombinant human basigin protein possesses tertiary structure and forms dimers.** *A*, comparison of the recombinant human basigin extracellular domain construct (rBSG) to full-length human basigin-1 and basigin-2. *N*, consensus asparagine-linked glycosylation sites; *SP*, signal peptide sequence; *TM*, transmembrane domain; *Cyto*, cytoplasmic domain. The N-terminal StrepTag II sequence and the C-terminal His$_6$ sequences of rBSG are shown. *B*, reducing and nonreducing SDS-PAGE of purified rBSG. The samples were heated at 95 °C in the presence or absence of 50 mM dithiothreitol (*DTT*) and resolved by SDS-PAGE. *C*, PFO-PAGE analysis of purified rBSG. *Left panel*, 2.5 μg of rBSG resolved by PFO-PAGE in the presence or absence of 100 mM dithiothreitol. *Right panel*, EMMPRIN pAb immunoblot of 0.25 μg of rBSG protein resolved by PFO-PAGE. Relative molecular mass standards (*Std*) are shown on the *left* for each gel.

erated (Table 1). Total RNA was isolated from HESC, CCL-2, C4-I, and C4-II cells, and oligo(dT) or random decamer-primed cDNA was generated using the Superscript III reverse transcriptase. cDNA sequences were amplified using PrimeStar HS polymerase, subcloned into the pBluescript II KS (−) plasmid vector, and sequenced at the Keck Biotechnology Center at the University of Illinois. Sequence analysis was performed using the Biology Workbench program.

RESULTS

The extracellular domain of basigin-2 was expressed periplasmically in *E. coli* as a polyhistidine-tagged fusion protein (Fig. 1*A*). Periplasmic expression exposes recombinant proteins to an oxidizing environment during the translocation through the periplasm, resulting in the formation of intramolecular disulfide bonds (34). The conserved cysteine residues flanking the immunoglobulin folds of basigin were anticipated to form disulfide bonds stabilizing the folded, native protein. To determine whether recombinant basigin (rBSG) possessed tertiary structure, rBSG was subjected to nonreducing and reducing SDS-PAGE. The results indicate that the periplasmically expressed rBSG migrates at a reduced molecular mass in a nonreducing SDS-PAGE (21 *versus* 23 kDa), demonstrating that the protein possesses a stable tertiary structure (Fig. 1*B*). Basigin is known to multimerize within the plasma membrane of cells, and this interaction is mediated in part by the first immunoglobulin domain (31). To test whether rBSG can form multimers in solution, PFO-PAGE was performed. The use of the detergent perfluorooctanoate in place of SDS during polyacrylamide gel electrophoresis allows for the maintenance of weak protein-protein interactions. Immunoblot analysis of rBSG protein resolved by PFO-PAGE demonstrated that rBSG forms dimers in solution only when the immunoglobulin domains of the protein are maintained in their nonreduced, native conformation (Fig. 1*C*).

The evidence that rBSG maintains a native conformation in solution suggested that the protein might function as a ligand to stimulate MMP expression in fibroblasts. To test this, human uterine fibroblasts (HESCs) (32) were treated with rBSG for 24 h, and the expression of MMP-1, -2, and -3 was determined using quantitative real time PCR. rBSG stimulated a dose-dependent increase for each MMP with the increases in MMP-1 and MMP-2 expression being statistically significant at 1 μg/ml

teins were eluted with 5 bed volumes of 2 mM D-Biotin in column buffer followed by 5 bed volumes of 100 mM glycine, pH 3.0. The glycine sample was neutralized with 1 M Tris, pH 9.5, and all of the fractions were concentrated and dialyzed into phosphate-buffered saline using 10,000 molecular weight cutoff centrifugal filters. Eluted proteins were resolved by 15% precast Tris-glycine SDS-PAGE (Bio-Rad) and either immunoblotted with streptavidin-HRP or stained in 0.1% Coomassie Brilliant Blue. For protein sequencing, purified biotinylated proteins were excised from Coomassie-stained SDS-PAGE gels and identified by MALDI-MS/MS using an Applied Biosystem 4700 Proteomics Analyzer. This work was performed at the Michael Hooker Proteomics Center at the University of North Carolina, Chapel Hill as part of the National Institutes of Health Specialized Cooperative Centers Program in Reproduction Research U54 program. The identities of the peptide sequences were determined by comparison with the nonredundant NCBI data base using the Mascot search engine.

Cloning and Sequencing of Basigin Isoforms 3 and 4—The nucleotide sequences corresponding to the sequenced peptides were used to map the exon-intron boundaries between the basigin isoforms using SPIDEY. Oligonucleotide primers complimentary to exons 1, 2, 5, and 10 of human basigin were gen-
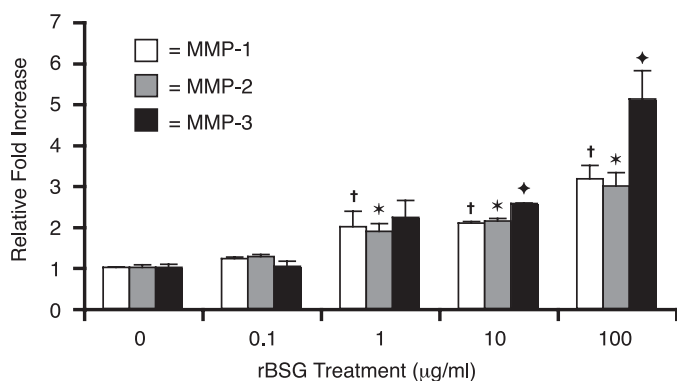
FIGURE 2. **rBSG stimulates MMP expression in HESC cells.** HESC cells were treated with the indicated concentrations of rBSG for 24 h, and the fold change in the expression of MMPs was determined by quantitative real time PCR. Results from three independent experiments are shown. The *error bars* represent standard errors. Analysis of variance was performed using Welch's analysis of variance and the statistical significance of the fold change was determined using Tukey's procedure ($\alpha < 0.05$). Significant gene expression changes over controls are indicated by symbols: †, MMP-1; *asterisk*, MMP-2; *black diamond*, MMP-3.

FIGURE 3. **Transfer of the SBED label from the rBSG ligand to live HESCs.** *A*, the diagram illustrates the features of the Sulfo-SBED heterotrifunctional cross-linking reagent used in these studies. The photoreactive aryl azide moiety allows for covalent attachment of the label to proteins within ~20 Å of the surface bound ligand. The NHS-ester group has a cleavable disulfide bond that allows transfer of the label from the ligand to the receptor following reduction with dithiothreitol. *B*, determination of the conditions used for label transfer to cell surface proteins. HESCs were treated with increasing amounts of SBED-labeled rBSG in serum-free medium for 10 min (*left panel*) or 30 min (*right panel*) prior to UV treatment. Biotinylated proteins were collected on Neutravidin beads, resolved by SDS-PAGE, and immunoblotted with Streptavidin-HRP. *C*, purification of biotinylated proteins following label transfer. SBED-labeled rBSG was used to label cells for 10 min, and biotinylated proteins were purified using monomeric avidin. *Control*, unlabeled HESC lysate; *Starting*, labeled cell lysate; *Unbound*, material not bound by avidin matrix; *Wash*, material washed from column; *Biotin*, proteins specifically eluted with biotin. *D*, Coomassie-stained SDS-PAGE of proteins eluted fractions from monomeric avidin and subjected to MALDI-MS/MS protein sequencing. The ~25-kDa protein from the labeled cells (*boxed*) is indicated. Insufficient material was present in the remainder of the gel for sequence identification of the remaining biotinylated proteins. The rBSG protein used for the labeling experiment is shown in the *far right lane*.

rBSG and significant for MMP-3 at 10 µg/ml (Fig. 2). As a control for the potential effects of lipopolysaccharide contamination of the rBSG protein on MMP expression, HESCs were treated with the amounts of lipopolysaccharide equal to that found in the rBSG treatments. The lipopolysaccharide treatments did not stimulate expression of MMPs (data not shown).

To identify the receptors responsible for rBSG binding, the rBSG protein was used as an affinity purification reagent in combination with the heterotrifunctional cross-linking agent Sulfo-SBED (Fig. 3*A*). Sulfo-SBED possesses an NHS-ester group for labeling of rBSG, an aryl azide group for UV light cross-linking of cell surface proteins to the rBSG ligand, and a biotin group for affinity purification of cross-linked protein complexes. A cleavable disulfide bond in the NHS-ester arm of Sulfo-SBED allows for the release of the cross-linker from the rBSG. Preliminary experiments to determine the amount of SBED-conjugated rBSG required for cell labeling indicated that the use of 50 µg/ml of rBSG for 10 min at 37 °C was sufficient to label the intact uterine fibroblasts (Fig. 3*B*), and all subsequent work employed these conditions for cell labeling. Streptavidin immunoblotting of monomeric avidin-purified protein complexes identified several biotinylated proteins including two major bands at 25 and ~50 kDa as well as three other less abundant proteins at 30, 100, and 120 kDa (Fig. 3*C*). The 25-kDa biotinylated protein, which was clearly visible by Coomassie staining (Fig. 3*D*), was subjected to tryptic digestion and MALDI-MS/MS protein identification. The peptide sequences were compared with the nonredundant NCBI data base using Mascot (35), and the results indicated that the peptides aligned with the human basigin-2 sequence (Fig. 4). However, peptide-1 (GTANIQLHGPPR) could not have been generated by tryptic digestion of human basigin-2 (Fig. 4, *bottom panel*). Probability-based scoring using Mascot indicated that the peptide-1 sequence best matched the translated mRNA sequence for a novel human basigin isoform named basigin-3 (accession number gi 38372921). Although the mRNA sequence for basigin-3 (RefSeq accession number NM_198590) and another closely related isoform, basigin-4 (RefSeq accession number
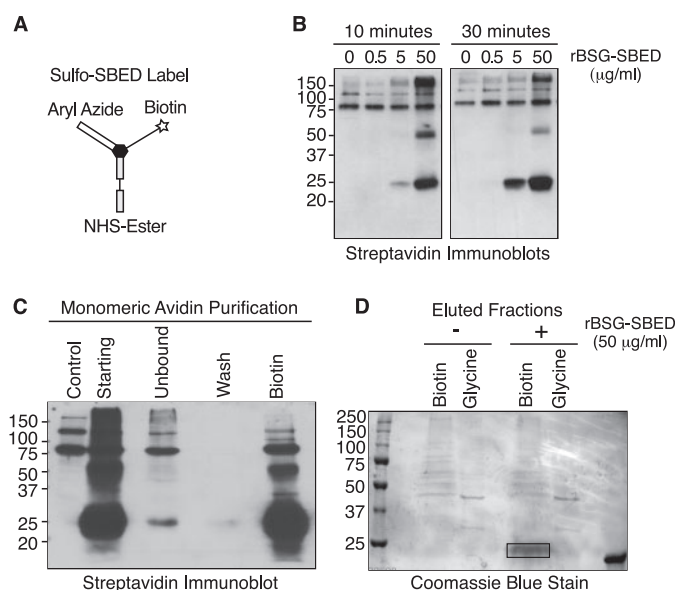
NM_198591), have been annotated within the RefSeq data base, no published reports have described these molecules.

The nucleotide sequences of basigin-3 and basigin-4 were compared with existing basigin sequences using the program SPIDEY. Mapping of the intron-exon boundaries identified a 255-bp exon sequence that is 958 bp upstream of the previously identified first exon of basigin. This exon is predicted to be expressed only by the basigin-3 and basigin-4 isoforms (Fig. 5*A*) and indicates that the human basigin gene is composed of 10 exons within human chromosome 19 covering 12.17 kb (NC_000019.8). Northern analysis for basigin-3 and basigin-4 using the first exon sequence as a probe did not detect any specific transcripts in uterine fibroblasts, nor in poly(A)+ RNA blots from 18 human tissues (data not shown). Therefore, reverse transcription-PCR using oligonucleotide primers corresponding to sequences within exons 1, 2, 5, and 10 of the basigin gene was performed (Fig. 5*B*). Amplification with primers specific to basigin-1 and basigin-2 (primers e and g) detected only the basigin-2 transcripts in the cell types tested (Fig. 5*C*). Amplification with primers specific to basigin-3 and basigin-4 (primers a and g) demonstrated the presence of both transcripts in the cell types tested (Fig. 5*D*). Quantitation of the

Sequenced Tryptic Peptides

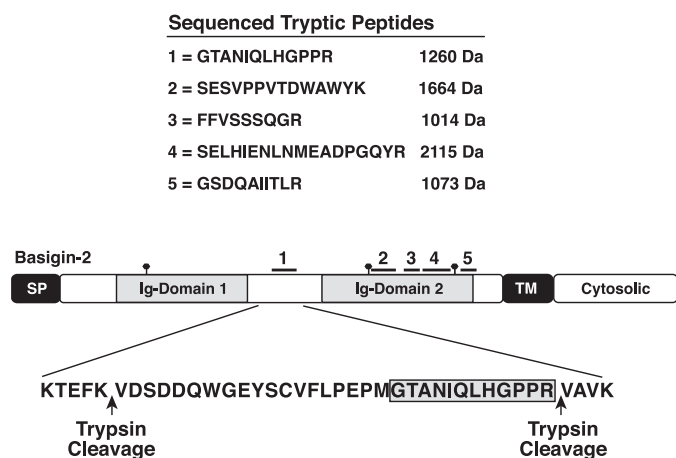|		
1 =	GTANIQLHGPPR	1260 Da
2 =	SESVPPVTDWAWYK	1664 Da
3 =	FFVSSSQGR	1014 Da
4 =	SELHIENLNMEADPGQYR	2115 Da
5 =	GSDQAIITLR	1073 Da

FIGURE 4. **MALDI-MS/MS sequencing of the 25-kDa protein identified it as basigin-3.** The amino acid sequences of the tryptic peptides from the purified protein are shown. Although the peptides align with the basigin-2 sequence, the 1260-Da peptide (GTANIQLHGPPR) could not have been generated as a tryptic peptide of basigin-2. The mass of basigin-2 peptide that contains this 1260-Da peptide sequence (*boxed*) is predicted to be 7026 Da. Therefore, probability-based scoring obtained using the Mascot search engine indicated that the sequenced protein best matched the translated mRNA sequence for human basigin-3 (accession number gi 38372921).
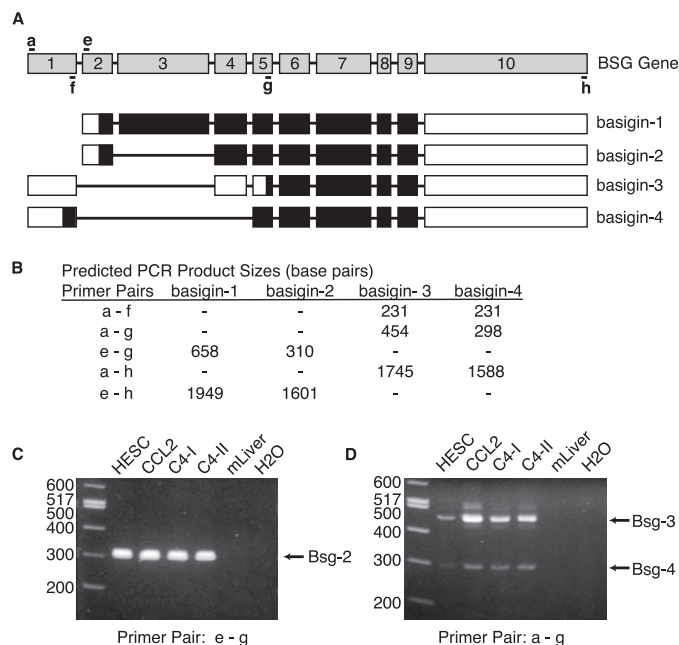

Predicted PCR Product Sizes (base pairs)

Primer Pairs	basigin-1	basigin-2	basigin-3	basigin-4
a - f	-	-	231	231
a - g	-	-	454	298
e - g	658	310	-	-
a - h	-	-	1745	1588
e - h	1949	1601	-	-

FIGURE 5. **Mapping and expression analysis of basigin splice variants.** *A*, intron-exon mapping of the human basigin gene sequence with the four mRNA sequences for human basigin using the program SPIDEY. The 10 exons of the human basigin gene are shown at *top* in *gray*, and the primers used in the study are indicated by *lowercase letters* (*a–e* are sense primers, and *f–h* are antisense primers). The *black boxes* correspond to the predicted open reading frames, and the *white boxes* correspond to untranslated regions of the transcripts. *B*, the predicted sizes of various reverse transcription-PCR products using primer pairs for each basigin isoform are indicated. *C*, PCR amplification of basigin-2 using cDNA from uterine fibroblast (HESC) and cervical carcinoma cell lines (CCL-2, C4-I, and C4-II). Control samples included PCR products from mouse liver cDNA (*mLiver*) and a no template control (*H2O*). Basigin-1 transcripts were not detected in any of the samples. *D*, PCR amplification of basigin-3 and basigin-4 from the cDNA samples used in *C*. To visualize the basigin-3 and basigin-4 PCR products, 10-fold more sample was loaded per lane in *D* (65 μl) than in *C* (6.5 μl).

relative transcript levels within each of the four cell lines was performed by densitometry using the ImageJ program. Following normalization for the amount of the PCR product loaded

per lane, we estimate that basigin-3 transcript levels are less than 3% of the basigin-2 levels in carcinoma cells and less than 1% of basigin-2 levels in fibroblasts. To confirm the identity of the amplified cDNAs, the PCR products were subcloned and sequenced. With the exception of a single nucleotide polymorphism in the basigin-3 from CCL-2 cells, the amplified sequences are identical to the existing RefSeq basigin sequences (data not shown). Alignment of the conceptually translated sequences for all four basigin isoforms (Fig. 6) demonstrated that they share a conserved core sequence (exons 5–10) and differ only in the extent of extracellular domain being expressed. One exception to this is the predicted 11-amino acid sequence at the N terminus of basigin-4 (MKQSDASPQER) that is unique to this isoform.

The proteomic data in Fig. 3 demonstrating the association of rBSG with basigin-3 suggests that these proteins interacted during the 10-min labeling period prior to UV treatment of the cells. However, basigin-3 does not possess a consensus signal peptide sequence normally required for membrane localization. To explain how the basigin-3 protein might interact with rBSG, protein localization studies were performed. The cells were separated into membrane and cytoplasmic fractions and used for immunoblot analysis. Control experiments using antibodies specific for the membrane protein caveolin-1 and the cytoplasmic protein SOS labeled the expected fractions (Fig. 7*A*). Similarly, basigin immunoblotting detected basigin-2 in the membrane fraction but did not detect the 25-kDa basigin-3 protein in either fraction (Fig. 7*A*, *middle panel*). The reverse transcription-PCR data in Fig. 5*D* suggested that basigin-3 might be expressed at levels too low to detect by immunoblotting of cell lysates. To detect low abundance isoforms, basigin proteins were immunoprecipitated from HESC fractions and then immunoblotted. The results show that in the absence of rBSG labeling, the 25-kDa protein corresponding to basigin-3 was detected exclusively in the cytoplasmic fraction (Fig. 7*B*, *arrowhead* in *left panel*). Repeating this procedure using fractions from labeled cells revealed a significant increase in the band(s) at ~25 kDa in both the membrane and cytoplasmic fractions. Because the relative molecular mass of rBSG (23 kDa) is nearly the same as that for basigin-3, the increase in basigin immunoreactivity at 23–25 kDa in both the membrane and cytoplasmic fractions from labeled cells (Fig. 7*B*, *right panel*) suggests that this increase is due to the presence of rBSG in both fractions. This result implies that rBSG associates with an unknown membrane receptor prior to being internalized into the cell. Previous reports have suggested that basigin-2 can function as the membrane receptor for soluble basigin protein, but attempts to directly test this hypothesis have not demonstrated this ability (20, 31). We tested this hypothesis by repeating the basigin immunoprecipitations from labeled HESC fractions, followed by immunoblotting with neutravidin-HRP to detect the transfer of the biotin label from the SBED-labeled rBSG to basigin-2 in the membrane fraction. The results revealed that a 50-kDa basigin protein in the membrane fraction was biotinylated only following treatment of uterine fibroblasts with SBED-labeled rBSG (Fig. 7*C*). Confirmation of the interaction between soluble rBSG and basigin-2 was demonstrated by repeating the label transfer experiment using the

```
           Exon 1              Exon 2                    Exon 3
         .           .         .          .          .           .
BSG1     MAAALFVLLGFALLGTHGASGA AGFVQAPLS QQRWVGGSVELHCEAVGSPVPEIQWWFE
BSG2     MAAALFVLLGFALLGTHGASGA A---------------------------------------
BSG3     --------------------------------------------------------------
BSG4  MKQSDASPQER----------------------------------------*---------------
```

```
         .          .          .          .           .
BSG1   GQGPNDTCSQLWDGARLDRVHIHATYHQHAASTISIDTLVEEDTGTYECRAS NDPDRNHLTRAPRVKWVR
BSG2   --------------------------------------------------------------------
BSG3   --------------------------------------------------------------------
BSG4   ------------------------------------------*-----------------------
```

```
                              Exon 4
         .            .          .          .          .
BSG1   AQAVVLVLEP GTVFTTVEDLGSKILLTCSLNDSATEVTGHRWLKGGVVLKEDALPGQKTEFK VDSDDQWG
BSG2   --------- GTVFTTVEDLGSKILLTCSLNDSATEVTGHRWLKGGVVLKEDALPGQKTEFK VDSDDQWG
BSG3   --------- -------------------------------------------------------
BSG4   --------- ------------------------------------------------------- VDSDDQWG
                    *  N-Gly
```

```
           Exon 5            .           Exon 6
         .          .                    .          .          .
BSG1   EYSCVFLPEPMGTANIQLH GP PRVKAVKSSEHINEGETAMLVCKSESVPPVTDWAWYKITDSEDK ALMNG
BSG2   EYSCVFLPEPMGTANIQLH GP PRVKAVKSSEHINEGETAMLVCKSESVPPVTDWAWYKITDSEDK ALMNG
BSG3   ----------MGTANIQLH GP PRVKAVKSSEHINEGETAMLVCKSESVPPVTDWAWYKITDSEDK ALMNG
BSG4   EYSCVFLPEPMGTANIQLH GP PRVKAVKSSEHINEGETAMLVCKSESVPPVTDWAWYKITDSEDK ALMNG
          *                                      *                         N-Gly
```

```
                              Exon 7
         .          .          .          .          .
BSG1   SESRFFVSSSQGRSELHIENLNMEADPGQYRCNGTSSKGSDQAIIT LRVRSHI AALWPFLGIVAEVLVLV
BSG2   SESRFFVSSSQGRSELHIENLNMEADPGQYRCNGTSSKGSDQAIIT LRVRSHI AALWPFLGIVAEVLVLV
BSG3   SESRFFVSSSQGRSELHIENLNMEADPGQYRCNGTSSKGSDQAIIT LRVRSHI AALWPFLGIVAEVLVLV
BSG4   SESRFFVSSSQGRSELHIENLNMEADPGQYRCNGTSSKGSDQAIIT LRVRSHI AALWPFLGIVAEVLVLV
                                         *N-Gly
```

```
                       Exon 8        Exon 9        Exon 10 - UTR
         .          .          .          .
BSG1   TIIFIY EKRRKPEDVLD DDDAGSAPL KSSGQHQND KGKNVRQRNSS
BSG2   TIIFIY EKRRKPEDVLD DDDAGSAPL KSSGQHQND KGKNVRQRNSS
BSG3   TIIFIY EKRRKPEDVLD DDDAGSAPL KSSGQHQND KGKNVRQRNSS
BSG4   TIIFIY EKRRKPEDVLD DDDAGSAPL KSSGQHQND KGKNVRQRNSS
```
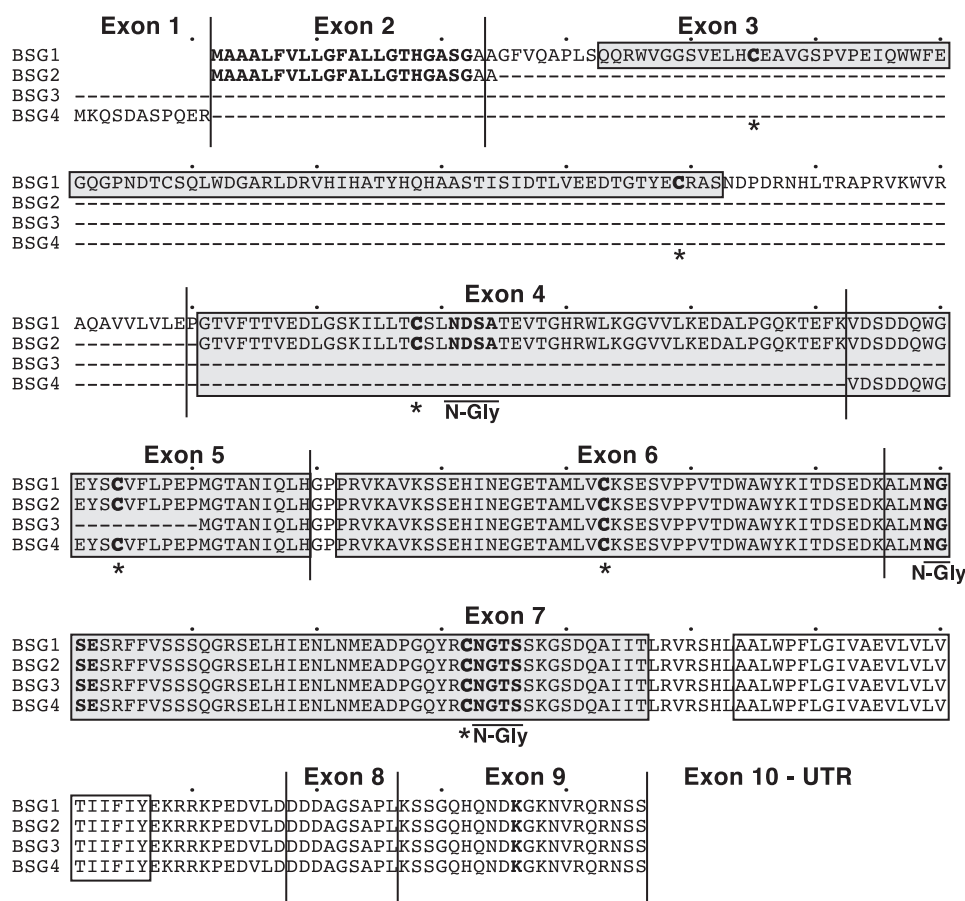
FIGURE 6. **Amino acid sequence alignment of the basigin isoforms.** The conceptually translated cDNA sequences for basigin-1, -2, -3, and -4 were aligned using the Biology Workbench program ClustalW. The exon boundaries are indicated and separated by *vertical lines*. The signal peptide sequence in exon 2 is shown in *bold letters*. The Ig-like domains are indicated with the *gray boxes*. The transmembrane domain in exon 7 is indicated with a *white box*. The single lysine residue that functions as a basolateral targeting motif is found in exon 9 (*bold K*). The tenth exon is not translated. Asparagine glycosylation sites are indicated by *bold letters* and *underlined* with *N-Gly*. The conserved cysteine residues necessary for stabilization of the immunoglobulin folds are indicated by *asterisks*.

cervical adenocarcinoma cell line CCL-2. Reciprocal precipitations from total cell lysates using the basigin monoclonal antibody and neutravidin beads were performed, and the precipitated proteins were immunoblotted with basigin pAb and streptavidin-HRP (See supplemental Fig. S2). The results show specific labeling of the 50-kDa basigin-2 protein as well as the 25-kDa basigin-3 protein.

To test the necessity for basigin-2 in rBSG-mediated cell signaling events, siRNAs were employed to knock down basigin-2 protein expression in HESCs. The cells were transfected with either negative control or basigin siRNAs for 48 h and treated with rBSG to measure changes in ERK1/2 phosphorylation. Treatment with rBSG activated the ERK1/2 signaling pathway in the negative control siRNA experiments, with maximal ERK phosphorylation occurring within 10–15 min of rBSG addition (Fig. 8*A, left panel*). Despite a nearly quantitative knockdown of basigin protein in the basigin siRNA-transfected cells, rBSG was still capable of stimulating ERK phosphorylation but to a lesser extent (Fig. 8*A, right panel*). Treatment of the HESCs with recombinant human EGF (rhEGF) stimulated the ERK signaling pathway regardless of the presence of endogenous basigin protein.

DISCUSSION

Many members of the immunoglobulin superfamily of proteins are known to function as cell adhesion molecules through homophilic molecular interactions on the surface of cells (28–30). Basigin-2 represents a prototypical form of the immunoglobulin superfamily having two extracellular Ig-like domains, a highly conserved transmembrane sequence, and a short cytoplasmic domain (reviewed in Refs. 3, 4, 36). Basigin-2 can form homo-oligomers (31) and associate with the integrins $\alpha3\beta1$ and $\alpha6\beta1$ within the plasma membrane in a *cis*-dependent manner (37). The N-terminal Ig-like domain (domain 1) of basigin is capable of mediating interactions between cancer cells and is responsible for the MMP stimulatory activity of basigin-treated cancer cells and fibroblasts (8, 27, 38). Basigin-2 is glycosylated at three asparagine residues within the Ig-like domains, and several reports indicate that this glycosylation is necessary for soluble basigin to stimulate signaling (27, 39). Together, the evidence suggests that basigin expressed on the surface of cells can function as a counter-receptor for basigin expressed on separate cells or for soluble glycosylated forms of basigin. Nevertheless, previous attempts to demonstrate such a direct interaction between basigin molecules on separate cells or between basigin proteins in solution have not been successful (20, 31).

In this paper, we present evidence that basigin-2 can function as a cell surface receptor for soluble basigin. This conclusion is based upon our label transfer results demonstrating the transfer of a biotin tag from a purified nonglycosylated rBSG protein to basigin-2 on uterine fibroblasts and cervical adenocarcinoma cells. The interaction between soluble basigin ligand and basigin-2 on the cell membrane results in the internalization of the basigin ligand and its subsequent interaction with a novel basigin isoform (basigin-3) within the cell. These interactions result in the activation of the ERK1/2 signaling pathway by an unknown mechanism, leading to increased expression of MMP-1, MMP-2, and MMP-3. However, our results suggest that basigin-2 may not be the only cell surface receptor for soluble basigin in stromal fibroblasts. The label transfer experiments reveal that at least five proteins interact with soluble rBSG. Furthermore, the siRNA knockdown of endogenous basigin greatly reduces ERK1/2 activation in response to rBSG stimulation but does not completely block activation. The abil-
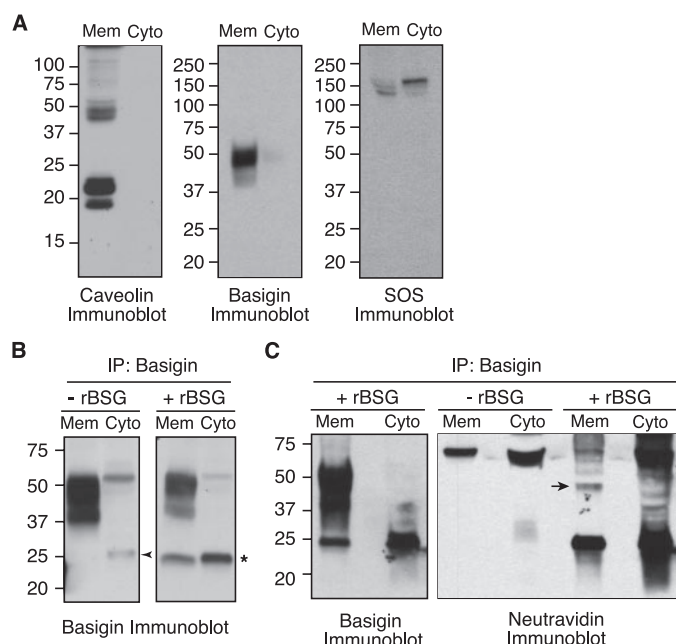
FIGURE 7. **Immunoprecipitation analysis of labeled HESC cell fractions reveals that basigin-2 is a membrane receptor for rBSG.** *A*, 20 μg of unlabeled HESC membrane (*Mem*) and cytosolic (*Cyto*) protein was resolved by SDS-PAGE and immunoblotted for the membrane protein caveolin-1, basigin, and the cytoplasmic protein SOS. Insufficient amounts of basigin-3 are present within 20 μg of each fraction to be detected. *B*, unlabeled HESC fractions (*left panel*) were immunoprecipitated with the basigin mAb P2C2 and immunoblotted with the R & D anti-EMMPRIN pAb. Note the presence of the 25-kDa basigin-3 protein exclusively in the cytosolic sample from unlabeled cells (*arrowhead*). Basigin immunoprecipitations (*IP*) from labeled cells (*right panel*) shows that the rBSG protein is present in both the membrane and cytosolic fractions (*asterisk*). The basigin-3 band could not be distinguished from the rBSG band in the cytosolic fraction because of the similarities in the size of both proteins. *C*, neutravidin immunoblotting shows that basigin-2 in the membrane is biotinylated in response to rBSG-SBED treatment. Basigin proteins were immunoprecipitated from HESC fractions using the mAb P2C2 and immunoblotted with either the EMMPRIN pAb (*left panel*) or neutravidin-HRP (*right panel*). A portion of the basigin-2 protein from the membrane is biotinylated (*arrow*).

FIGURE 8. **Basigin protein knockdown in HESCs does not eliminate rBSG-mediated ERK activation.** HESCs were reverse-transfected with either the negative control 1 siRNA oligonucleotide (*left panels*) or the basigin siRNA oligonucleotide (*right panels*). The basigin siRNA sequences used were: sense strand, GCUACACAUUGAGAACCUGtt; antisense strand, CAGGUUCUCAAU-GUGUAGCtc. *A*, HESCs were treated with 10 μg/ml rBSG for the times indicated, and equivalent amounts of cell lysate were resolved by SDS-PAGE. Immunoblotting was performed using the antibodies indicated on the right, and all of the immunoblots were processed under identical conditions. The immunoblots in the *left* and *right panels* were exposed to the same piece of film and exposed for the same amount of time. An *asterisk* indicates the rBSG protein. *B*, HESCs were transfected as indicated in *A* and treated with 100 ng/ml recombinant human EGF. Note that basigin knockdown does not affect rhEGF-mediated ERK activation in HESCs. This work was performed twice with identical results.

ity of a nonglycosylated form of basigin to induce MMP expression in fibroblasts contradicts previous studies indicating that *N*-glycosylation of basigin is necessary for its stimulatory activity (27, 39). One possible explanation for the biological activity of rBSG is the evidence for both tertiary and quaternary structure of the protein. Periplasmic expression of rBSG exposes the protein to an oxidative environment allowing for the formation of intramolecular disulfide bonds during translocation into the periplasm (34). Reducing and nonreducing SDS-PAGE analysis confirmed that rBSG possesses tertiary structure as evidenced by the altered mobility of the protein in the absence of reductant. Furthermore, maintenance of the disulfide-stabilized structure of rBSG allows it to form dimers in solution as shown in the PFO-PAGE analysis. We hypothesize that the formation of rBSG dimers promotes binding to cell surface receptors to promote receptor aggregation and activation of signaling events leading to increased MMP expression. The results from a previous study support this mechanism for basigin-mediated signaling where it was demonstrated that cross-linking of basigin-2 on the surface of human lung fibroblasts enhanced basigin-stimulated MMP-3 expression (40).
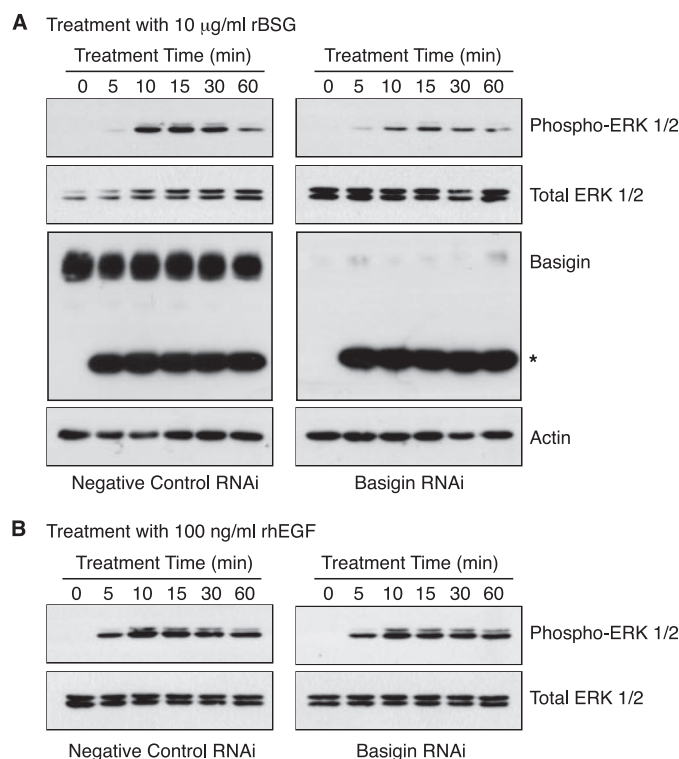
The previous lack of evidence for direct homophilic interactions between soluble basigin and basigin-2 on the cell surface suggested that basigin-2 might not be a receptor for soluble basigin. In a nonbiased attempt to identify the receptor for soluble basigin, we utilized the rBSG protein as an affinity probe. The heterotrifunctional cross-linking agent Sulfo-SBED was used to covalently link the surface bound rBSG protein to putative receptors. The length of the spacer arms linking the aryl azide and biotin moieties on SBED should result in the cross-linking of any protein within ~20 Å of the bound rBSG. Initial label transfer experiments demonstrated labeling of fibroblast cells within 10 min of rBSG addition, and monomeric avidin purification experiments subsequently showed that at least five proteins of 25, 30, 50, 100, and 120 kDa were biotinylated. Proteomic sequencing of the eluted proteins and probability-based scoring using the Mascot search engine unambiguously identified the major biotinylated protein at 25 kDa as the novel basigin isoform, basigin-3. The protein sequence data for the four other less abundant proteins was not obtained. Characterization of basigin-3 expression in both fibroblasts and carcinoma cells indicated that this isoform is present at relatively low levels and is expressed

within the cytoplasm. Therefore, we conclude that basigin-3 cannot be a cell surface receptor for soluble basigin.

The label transfer data presented in Fig. 3*C* suggests that the four biotinylated proteins at 30, 50, 100, and 120 kDa might represent candidate cell surface receptors for soluble basigin. The 50-kDa protein was also present in both neutravidin pulldowns and basigin immunoprecipitations from labeled fibroblasts and carcinoma cells (see supplemental Fig. S2 and Figs. 3*B* and 7*C*). Basigin immunoprecipitations from fibroblast cell fractions further demonstrated that the biotinylated 50-kDa protein is present only within the membrane fraction. Based upon this data, we conclude that this protein is basigin-2 and propose that it functions as a cell surface receptor for soluble basigin. To test the necessity of basigin-2 for rBSG-mediated ERK activation, RNA interference studies were performed. Knockdown of basigin-2 protein in fibroblasts markedly reduced ERK signaling in response to rBSG but did not completely eliminate it. Therefore, we conclude that basigin-2 is important, but not necessary, for ERK signaling in response to treatment with rBSG. Together, the data suggest that there are additional cell surface receptors for soluble basigin that have not yet been identified.

The transfer of a biotin tag from rBSG to basigin-3 during the label transfer procedure implies that basigin-3 must associate with rBSG during the 15-min labeling procedure (10 min of labeling and 5 min of UV cross-linking). We propose that binding of soluble basigin ligand to basigin-2 on the cell surface stimulates receptor-ligand internalization in a manner similar to other cell surface receptors (41), leading to subsequent interactions between rBSG and basigin-3 within the cell. Previous work by Yurchenko *et al.* (42) has demonstrated that basigin-2 can function as a signaling receptor for cyclophilin A. Future studies will be needed to fully characterize the mechanism of basigin-mediated signaling and receptor-ligand internalization.

This study demonstrates that four isoforms of basigin are transcribed from the basigin gene. The two isoforms identified in this study, basigin-3 and basigin-4, are splice variants that utilize an additional 255-bp exon that is 958 bp upstream from the previously identified first exon of the basigin gene. The original studies that mapped the human basigin gene concluded that the gene was composed of 8 exons that span 10.8 kb on the proximal arm of chromosome 19 (19). Subsequent studies revealed that the human basigin gene possessed a previously unidentified 348-bp exon within the first intronic sequence. This exon, described by Hanna *et al.* (20), codes for an additional extracellular immunoglobulin-like domain ("domain 0") in basigin isoform 1 and is expressed only in the retina (23). Our data add to these previous findings by demonstrating that the basigin gene contains an additional 255-bp exon upstream of the previously identified first exon. Therefore, the human basigin gene is composed of a total of 10 exons covering 12.17 kb on the proximal arm of human chromosome 19.

In conclusion, the data presented herein demonstrate that a nonglycosylated recombinant human basigin (rBSG) protein can interact with basigin-2 at the cell surface, resulting in the activation of the ERK1/2 signaling pathway leading to increased expression of MMP-1, MMP-2, and MMP-3 in uterine fibro-

blasts. The label transfer and basigin siRNA knockdown data also suggest that additional unidentified cell surface receptors for soluble basigin exist. This study also identifies two novel isoforms of basigin (basigin-3 and basigin-4), and we present evidence indicating that basigin-3 in the cytoplasm of uterine fibroblasts interacts with the internalized basigin receptor-ligand complex. At this time, the functions for basigin-3 and basigin-4 proteins are not known. It should be noted that the evolutionarily conserved basigin transmembrane domain sequence present within all four basigin isoforms contains a charged glutamic acid residue, as well as leucine zipper-like sequences (reviewed in Ref. 3). It is possible that these novel basigin isoforms might be involved in additional protein-protein interactions within the cell.

REFERENCES

1. Liotta, L. A., and Kohn, E. C. (2001) *Nature* **411,** 375–379
2. Gabison, E. E., Hoang-Xuan, T., Mauviel, A., and Menashi, S. (2005) *Biochimie. (Paris)* **87,** 361–368
3. Yan, L., Zucker, S., and Toole, B. P. (2005) *Thromb. Haemostasis* **93,** 199–204
4. Muramatsu, T., and Miyauchi, T. (2003) *Histol. Histopathol.* **18,** 981–987
5. Biswas, C. (1982) *Biochem. Biophys. Res. Commun.* **109,** 1026–1034
6. Biswas, C. (1984) *Cancer Lett.* **24,** 201–207
7. Nabeshima, K., Lane, W. S., and Biswas, C. (1991) *Arch. Biochem. Biophys.* **285,** 90–96
8. Biswas, C., Zhang, Y., DeCastro, R., Guo, H., Nakamura, T., Kataoka, H., and Nabeshima, K. (1995) *Cancer Res.* **55,** 434–439
9. Seulberger, H., Unger, C. M., and Risau, W. (1992) *Neurosci. Lett.* **140,** 93–97
10. Fossum, S., Mallett, S., and Barclay, A. N. (1991) *Eur. J. Immunol.* **21,** 671–679
11. Altruda, F., Cervella, P., Gaeta, M. L., Daniele, A., Giancotti, F., Tarone, G., Stefanuto, G., and Silengo, L. (1989) *Gene (Amst.)* **85,** 445–451
12. Nehme, C. L., Cesario, M. M., Myles, D. G., Koppel, D. E., and Bartles, J. R. (1993) *J. Cell Biol.* **120,** 687–694
13. Fadool, J. M., and Linser, P. J. (1993) *Dev. Dyn.* **196,** 252–262
14. Seulberger, H., Lottspeich, F., and Risau, W. (1990) *EMBO J.* **9,** 2151–2158
15. Kasinrerk, W., Fiebiger, E., Stefanova, I., Baumruker, T., Knapp, W., and Stockinger, H. (1992) *J. Immunol.* **149,** 847–854
16. Spring, F. A., Holmes, C. H., Simpson, K. L., Mawby, W. J., Mattes, M. J., Okubo, Y., and Parsons, S. F. (1997) *Eur. J. Immunol.* **27,** 891–897
17. (1996) *Tissue Antigens* **48,** 352–508
18. Kaname, T., Miyauchi, T., Kuwano, A., Matsuda, Y., Muramatsu, T., and Kajii, T. (1993) *Cytogenet. Cell Genet.* **64,** 195–197
19. Guo, H., Majmudar, G., Jensen, T. C., Biswas, C., Toole, B. P., and Gordon, M. K. (1998) *Gene (Amst.)* **220,** 99–108
20. Hanna, S. M., Kirk, P., Holt, O. J., Puklavec, M. J., Brown, M. H., and Barclay, A. N. (2003) *BMC Biochem.* **4,** 17
21. Miyauchi, T., Masuzawa, Y., and Muramatsu, T. (1991) *J. Biochem. (Tokyo)* **110,** 770–774
22. Deora, A. A., Gravotta, D., Kreitzer, G., Hu, J., Bok, D., and Rodriguez-Boulan, E. (2004) *Mol. Biol. Cell* **15,** 4148–4165
23. Ochrietor, J. D., Moroz, T. P., van Ekeris, L., Clamp, M. F., Jefferson, S. C., deCarvalho, A. C., Fadool, J. M., Wistow, G., Muramatsu, T., and Linser,

P. J. (2003) *Investig. Ophthalmol. Vis. Sci.* **44,** 4086 – 4096

24. Tang, W., Chang, S. B., and Hemler, M. E. (2004) *Mol. Biol. Cell* **15,** 4043– 4050

25. Sidhu, S. S., Mengistab, A. T., Tauscher, A. N., LaVail, J., and Basbaum, C. (2004) *Oncogene* **23,** 956 –963

26. Caudroy, S., Polette, M., Nawrocki-Raby, B., Cao, J., Toole, B. P., Zucker, S., and Birembaut, P. (2002) *Clin. Exp. Metastasis* **19,** 697–702

27. Sun, J., and Hemler, M. E. (2001) *Cancer Res.* **61,** 2276 –2281

28. Miller, J., Knorr, R., Ferrone, M., Houdei, R., Carron, C. P., and Dustin, M. L. (1995) *J. Exp. Med.* **182,** 1231–1241

29. Zhou, H., Fuks, A., Alcaraz, G., Bolling, T. J., and Stanners, C. P. (1993) *J. Cell Biol.* **122,** 951–960

30. Tomschy, A., Fauser, C., Landwehr, R., and Engel, J. (1996) *EMBO J.* **15,** 3507–3514

31. Yoshida, S., Shibata, M., Yamamoto, S., Hagihara, M., Asai, N., Takahashi, M., Mizutani, S., Muramatsu, T., and Kadomatsu, K. (2000) *Eur. J. Biochem.* **267,** 4372– 4380

32. Krikun, G., Mor, G., Alvero, A., Guller, S., Schatz, F., Sapi, E., Rahman, M., Caze, R., Qumsiyeh, M., and Lockwood, C. J. (2004) *Endocrinology* **145,** 2291–2296

33. Ramjeesingh, M., Huan, L. J., Garami, E., and Bear, C. E. (1999) *Biochem. J.* **342,** 119 –123

34. Nakamoto, H., and Bardwell, J. C. (2004) *Biochim. Biophys. Acta* **1694,** 111–119

35. Perkins, D. N., Pappin, D. J., Creasy, D. M., and Cottrell, J. S. (1999) *Electrophoresis* **20,** 3551–3567

36. Gabison, E. E., Mourah, S., Steinfels, E., Yan, L., Hoang-Xuan, T., Watsky, M. A., De Wever, B., Calvo, F., Mauviel, A., and Menashi, S. (2005) *Am. J. Pathol.* **166,** 209 –219

37. Berditchevski, F., Chang, S., Bodorova, J., and Hemler, M. E. (1997) *J. Biol. Chem.* **272,** 29174 –29180

38. Nabeshima, K., Suzumiya, J., Nagano, M., Ohshima, K., Toole, B. P., Tamura, K., Iwasaki, H., and Kikuchi, M. (2004) *J. Pathol.* **202,** 341–351

39. Guo, H., Zucker, S., Gordon, M. K., Toole, B. P., and Biswas, C. (1997) *J. Biol. Chem.* **272,** 24 –27

40. Li, R., Huang, L., Guo, H., and Toole, B. P. (2001) *J. Cell Physiol.* **186,** 371–379

41. McNiven, M. A. (2006) *Trends Cell Biol.* **16,** 487– 492

42. Yurchenko, V., Zybarth, G., O'Connor, M., Dai, W. W., Franchin, G., Hao, T., Guo, H., Hung, H. C., Toole, B., Gallay, P., Sherry, B., and Bukrinsky, M. (2002) *J. Biol. Chem.* **277,** 22959 –22965